AIAA 79-1499R

Experimental Measurements of Shock/Boundary-Layer Interaction on a Supercritical Airfoil

Kenneth P. Burdges*
Lockheed-Georgia Company, Marietta, Georgia

A recent investigation of the shock/boundary layer interaction region of a state-of-the-art supercritical airfoil in the Lockheed-Georgia Compressible Flow Wind Tunnel is summarized. The test apparatus is a half airfoil model, mounted on the floor of the tunnel, which provides a boundary layer with proper upstream history from stagnation point through the shock wave to the trailing edge. A four-tube probe traversed the boundary layer in the vicinity of the shock wave. Measurements were made at all flow boundaries to provide boundary conditions for Navier-Stokes calculations of the entire flowfield.

Nomenclature

c = airfoil chord length
C_f = skin friction coefficient
C_l = lift coefficient
C_p = pressure coefficient
M = Mach number
p = pressure
R_{N_c} = Reynolds number based on chord
SBLI = shock/boundary-layer interaction
U = chordwise velocity
x = chordwise coordinate, measured from leading edge
y = coordinate normal to the surface
γ = ratio of specific heats
δ = boundary layer thickness
δ^* = boundary layer displacement thickness
θ = boundary layer momentum thickness
ρ = density
τ = skin friction
ν = kinematic viscosity

Subscripts

e = boundary layer edge conditions
w = wall condition
τ = skin friction
∞ = ambient conditions

I. Introduction

WITH the advent of supercritical airfoil design concepts in the 1960's, the trend over the last decade has been to design thicker and more highly-loaded airfoils for transport aircraft cruising at transonic speeds. As a result of this trend, it has become increasingly more difficult to predict the performance of these airfoils. This difficulty arises because the boundary layer over the aft portion of a thick, highly-loaded supercritical airfoil approaches separation and cannot be adequately predicted by boundary-layer theory. This problem is further aggravated by the presence of a shock wave on the airfoil interacting with the turbulent boundary layer. Boundary-layer theory is also inadequate to describe the flow phenomena in the shock/boundary layer interaction (SBLI) region when the shock wave is of substantial strength.

To improve the theoretical analysis capability for airfoils experiencing strong inviscid-viscous flow interactions, considerable effort is being expended to model those flows with the Navier-Stokes equations.[1] Current research efforts center around solution algorithm development and turbulence modeling investigations. For the Navier-Stokes mathematical modeling research to continue to make progress, a substantial experimental data-base is needed. Data are required for better understanding of the SBLI flow physics, to develop flow models, and to correlate theoretical codes.

Various approaches have been used over the years to establish an experimental data base for transonic shock/boundary-layer interactions. One of the earliest approaches to obtaining SBLI data was to use a shock-wave generator in a supersonic flowfield (Fig. 1a) to produce a shock wave which impinged on a flat plate.[2-4] This approach provided considerable information on interaction phenomena but had the obvious disadvantage of being a considerable simplification of a SBLI on an airfoil.

A second approach to obtaining fundamental SBLI data has been to position a normal shock wave in a wind-tunnel test section and study its interaction with the tunnel wall boundary.[5,6] A schematic of this approach is shown in Fig. 1b. This approach has the disadvantage that it does not provide the same type flowfield above the boundary layer that would be encountered above an airfoil.

To more closely approximate an airfoil-type SBLI, two-dimensional bumps mounted on a wind-tunnel wall (Fig. 1c) have been investigated.[7,8] This approach has the disadvantage of the wind-tunnel boundary layer being superimposed upon the model boundary layer. The wind-tunnel boundary layer has an uncertain origin, such that Reynolds number and upstream history are unlike those of an airfoil layer. The state of the airfoil boundary layer is important since SBLI phenomena on supercritical airfoils are highly sensitive to Reynolds number variations. Further, most bump configurations tested to date do not approximate advanced supercritical airfoil shapes. The airfoil shape is important since it governs the type of SBLI that will be produced (Class A or Class B[9]).

Attempts at providing experimental data for SBLI on supercritical airfoils have been recently reported by Sobieczky et al.[10] and Hurley et al.[11] These experiments were conducted on small-scale airfoil models at low Reynolds numbers and were limited in scope. Since the character of the SBLI may change going from tests at low values of Reynolds number to flight conditions at high values of Reynolds number, it is imperative that flight Reynolds number SBLI data be obtained. Additional in-depth flowfield and boundary-layer measurements are needed on supercritical airfoil shapes at transonic speeds over a wide range of Reynolds numbers to adequately support the development of advanced theoretical codes.

Presented as Paper 79-1499 at the AIAA 12th Fluid and Plasma Dynamics Conference, Williamsburg. Va., July 23-25, 1979; submitted Oct. 2, 1979; revision received Sept. 22, 1980. Copyright © American Institute of Aeronautics and Astronautics, Inc., 1980. All rights reserved.

*Scientist.

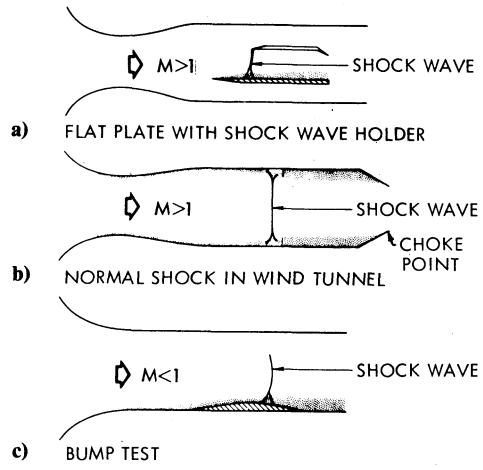

Fig. 1 Configurations for investigation of normal shock interaction with boundary layer.

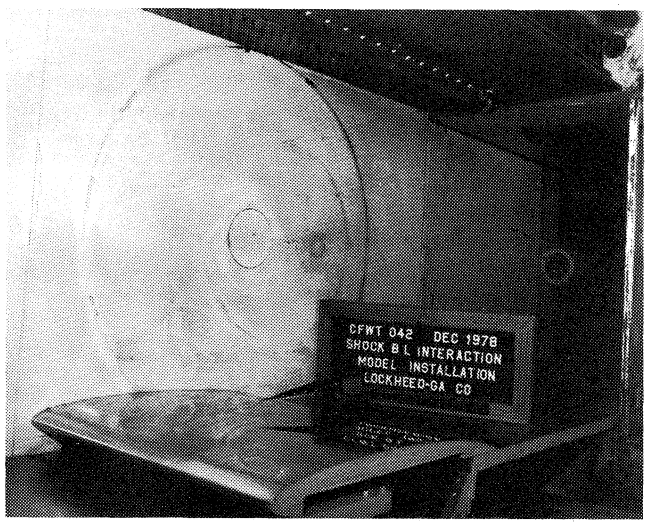

Fig. 2 Shock/boundary-layer interaction apparatus.

In 1977, Lockheed-Georgia Company initiated a program to obtain an experimental data-base that would adequately support the development of advanced theoretical codes for the analysis of supercritical airfoils encountering strong shock-wave/boundary-layer interactions. The initial step in this program was to design an experiment that would yield the desired results and did not have the disadvantages of the experimental approaches discussed above. The experimental apparatus that evolved from this work is shown in Fig. 2 mounted in the Lockheed Compressible Flow Wind Tunnel.

It is the objective of this paper to describe the SBLI experimental apparatus shown in Fig. 2, and to present experimental aerodynamic results obtained with the apparatus for a condition representative of the supercritical airfoil design point.

II. Experimental Tests

Experimental Apparatus

Design Considerations

In the development of the experimental apparatus several constraints on the design were imposed:

A supercritical airfoil shape was to be used.

Apparatus had to produce results indicative of airfoil flows.

Flow conditions had to include: 1) variable angle of attack; 2) Reynolds numbers ranging from conventional wind-tunnel values up to flight conditions of 90 million; and 3) transonic flows.

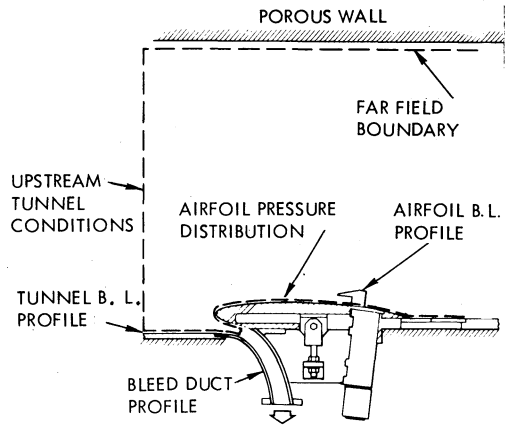

Fig. 3 Summary of experimental measurements.

Fig. 4 Sketch of LG4-612 airfoil.

Capability to measure: 1) airfoil pressure distributions; 2) mean boundary-layer velocity profiles; 3) turbulent velocity fluctuations; 4) surface skin-friction; and 5) wind-tunnel wall boundary data.

A sketch of the experimental apparatus selected to meet these constraints is shown in Fig. 3.

The apparatus of Fig. 3 consists of a half-airfoil model mounted on the floor of the Lockheed CFWT. The wind-tunnel floor boundary layer is removed via a separate bleed system so that a new boundary layer will begin at the airfoil leading-edge stagnation point. This ensures an airfoil-type flow over the model. The instrumentation includes surface static pressures on tunnel walls and model, boundary-layer traversing probe, tunnel pressure rails, and wall-mounted flow angle probes.

In the paragraphs to follow, the detailed design of the experimental apparatus will be described.

Airfoil Model

The airfoil selected for investigation was the Lockheed-Georgia Company LG4-612 airfoil shown sketched in Fig. 4. This airfoil was designed using supercritical design concepts and has been investigated previously over a wide range of Mach numbers and Reynolds numbers in the Lockheed CFWT.[12]

Experimental results on the LG4-612 airfoil[12] indicate that the flow characteristics peculiar to a supercritical airfoil are present. At design conditions of $M=0.76$ and $C_l=0.6$, a mild shock wave is present near the mid-chord region of the airfoil upper surface as shown in Fig. 5. At off-design conditions slightly higher than the design point, a separation bubble (Class A SBLI) appears to form at the foot of the shock wave. For off-design conditions considerably above the design point, a shock-induced trailing-edge separation is present (Class B SBLI). From these observations it can be concluded that the LG4-612 supercritical airfoil is a suitable subject for a shock/boundary-layer interaction investigation.

A half-airfoil model consisting of the leading-edge and upper surface of the LG4-612 airfoil is shown in Fig. 2 mounted on the floor of the Lockheed CFWT. The model completely spans the 20 in. width of the tunnel and model chord is 20 in. The model was constructed of stainless steel with an exceptionally smooth finish.

The half-airfoil model was mounted on top of a one-in. high bleed duct attached to the floor of the wind-tunnel (see

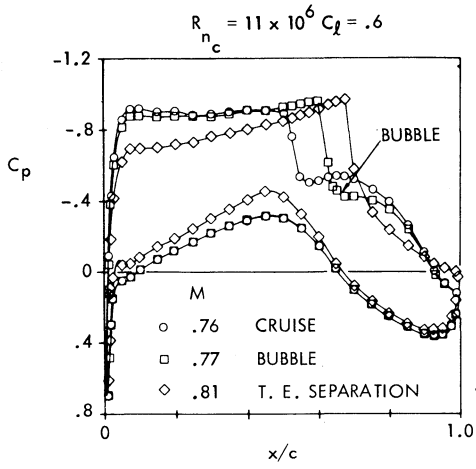

Fig. 5 Pressure distribution of LG4-612 at various Mach numbers.

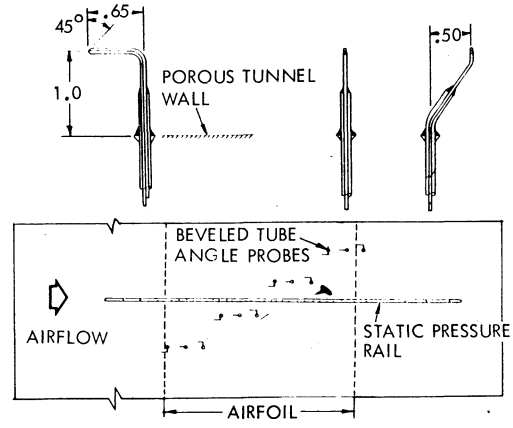

Fig. 6 Tunnel upper wall instrumentation.

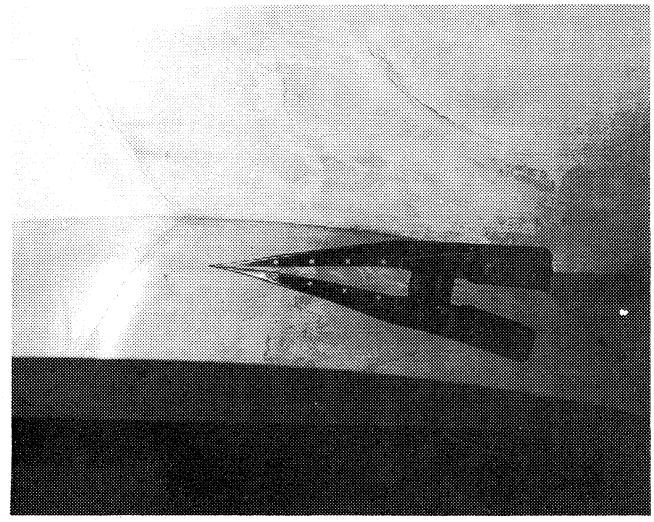

Fig. 7 Boundary layer probe installation.

sketch in Fig. 3). The bleed duct spans the tunnel and removes the floor boundary-layer via connection to a modulated atmospheric discharge system. Attachment of the model to the bleed duct is at 10% chord on the airfoil lower surface. The resulting leading-edge and upper surface provide a good simulation of the airfoil flow beginning at the stagnation point and moving rearward over the airfoil upper surface. The lower surface flow aft of the stagnation point is taken down the bleed duct.

Angle of attack of the airfoil can be varied over a limited range. This is accomplished by lowering the floorplate aft of the airfoil trailing-edge and rotating the airfoil about a flexture point built into the model lower surface at 5% chord as can be seen in Fig. 3.

Test Facility

The Lockheed CFWT is a blow-down transonic wind-tunnel with a test section that is 20 in. wide, 28 in. tall, and 72 in. long. The facility is capable of simulating Reynolds numbers of 5 to 55 million/ft. The Mach number can be varied over a range from 0.2 to 1.2. For the half model tests, the test section consisted of a solid floor and side walls, and a variable porosity top wall.

The variable porosity test-section upper wall consists of two adjacent perforated plates with 0.25 in. diam holes slanted 60 deg from the vertical. The porosity may be varied from closed to 10% open by moving the outside shutter plate upstream to misalign the perforations.

Instrumentation

The instrumentation for this experiment was selected to provide the data needed for continued development and correlation of advanced Navier-Stokes analysis codes. The kinds of data required are depicted in Fig. 3, and the instrumentation used for their measurement is discussed below.

Airfoil Static Pressure

The airfoil pressure distribution was measured with 53 static-pressure orifices located in a line half-way between the midspan of the model and the wall to avoid disturbing the boundary layer along the airfoil centerline where boundary-layer probe measurements were to be made.

Tunnel Upper-Wall Measurements

For theoretical code development, it is desirable that the experimental data-base be indicative of free-air results without spurious wind-tunnel wall effects. Since interference-free data are not achievable, it was decided to eliminate the wall effects problem by measuring the flow conditions at the walls and using these as input to the theoretical codes in the form of boundary conditions.

The flowfield boundary conditions for the Navier-Stokes codes require a knowledge of both velocity magnitude and direction. To obtain this type of data, both wall-static rail and flow-angle wall probes were used. A sketch of the upper-wall instrumentation is shown in Fig. 6. The velocity magnitude was obtained from the static rail shown in Fig. 6. The rail orifices were mounted 1.3 chord lengths above the model chordline.

Twelve flow-angle probes of the type shown in Fig. 6 were constructed for measuring the flow angle at the wall. The probes were made of beveled hypodermic tubing fitted through the tunnel porous wall in place of bolts that held the shutter plates together. Since the probes were total pressure devices, they were staggered across the test section to prevent the wake from one probe from interfering with the measurements of other downstream probes.

Tunnel Floor Measurements

Measurements of the static pressure along the solid wind-tunnel floor ahead of the airfoil were made at six locations beginning at a distance of 0.3 chords ahead of the model. Pressure measurements were also obtained across the tunnel floor boundary-layer removal duct. For the duct measurements, a six-tube pitot rake was used.

Boundary-Layer Velocity Profiles

Since it was desired to measure the mean flow quantities—total pressure, static pressure, and flow angle—through the boundary layer, a miniature four-tube probe was selected. To minimize calibration and to minimize interference to the flow,

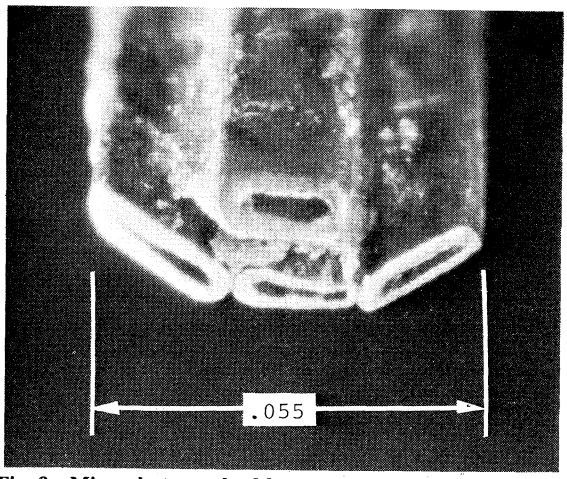

Fig. 8 Microphotograph of four-tube boundary-layer probe.

Fig. 9 Probe calibration apparatus.

a thin probe blade with four tubes at the tip was chosen, which was driven vertically through the boundary layer by a traversing mechanism. The probe could be positioned at five different x/c locations. A photograph of the assembled probe is shown in Fig. 7. The probe was electrically insulated from the support stem so that contact of the tip with the airfoil surface could be detected by electric circuit. The probe tip was tangent to the airfoil surface for all longitudinal positions.

The probe traverse was driven by a stepper motor. A photoelectric encoder determined rotational position of the motor drive shaft. Position of the probe was determined by counting the number of shaft encoder pulses as the probe was driven toward the surface. Each encoder pulse was equivalent to 0.002 in. of probe movement and contact with the surface was used to establish the absolute position.

The four-tube probe tip with 0.002 in. high openings is shown in the photograph of Fig. 8. The beveled side tubes were used to measure static pressure variation through the boundary layer. The beveled top tube was used to measure vertical-flow angle. The bottom tube was used to measure total pressure.

Instrumentation Calibration

An open-jet probe calibration apparatus, shown in Fig. 9, was built and used for calibration of all probes. Position and angular movements of the probe during calibration were made by a machinist's rotary table. The same dry-air supply that powers the Lockheed CFWT was used to eliminate contamination problems.

Each of the twelve flow-angle probes mounted on the upper tunnel wall was calibrated in the open-jet as a function of flow angle at several Mach numbers from 0.2 to 1.0. The flow angle probes were then installed in the CFWT and tested without the airfoil present to establish an installation angle for each probe. The static pressure rail was also installed and calibrated at this time.

The miniature four-tube, boundary-layer probe was calibrated as a function of yaw and pitch angle for several Mach numbers from 0.2 to 1.0. Extension of the probe static pressure calibration of supersonic conditions was accomplished by use of airfoil test data obtained far ahead of the shock wave and above the boundary layer.

Test Conditions

Tests of the half airfoil were conducted over the Mach number range from 0.6 to 0.78 at a geometric angle of attack of 0 deg. Although the experiment apparatus and test facility allow tests up to 90 million, the present tests were limited to a chord Reynolds number of 11×10^6. The modulator valve located in the tunnel boundary layer removal system was operated at 60 to 100%. Wind-tunnel wall porosity on the upper wall was varied from 2-8%. Boundary layer measurements were made in the 40 to 60% chord range which covers the shock/boundary-layer interaction region for cruise conditions.

Transition

The model was tested with roughness particles located on the upper surface at 5% chord to provide a fully turbulent flow over the model. The roughness strips were 0.0025 chords wide and consisted of Ballotini glass beads 0.00027 chords high set in a plastic adhesive.

Data Reduction

All pressure data, with the exception of the boundary-layer probe was acquired on scanivalves. The probe data was acquired with a separate transducer for each of the four tubes. Instantaneous tunnel conditions, measured at the same time each pressure measurement was made, were used to reduce all pressure measurements to standard coefficient form. Tunnel conditions for the run were taken as the average of all instantaneous measurements.

Although static pressure and flow-angle variations were obtained through the boundary layer, the data was not sufficiently reduced at the time of publication to be used in mean velocity-profile computation. Therefore, it was assumed that the static pressure was constant throughout the boundary layer. The value of static pressure was obtained from airfoil-surface static-pressure measurements. For the cruise SBLI results to be presented, where the shock is relatively weak, the assumption of constant static pressure is reasonable. The edge of the boundary layer was determined by a computer interpolation for the 99.5% U_e location from the set of local velocities. Values of δ^*/c and θ/c were obtained by numerical integration.

Values of C_f were determined by assuming the data would conform to law of the wall form.

$$\frac{U}{U_\tau} = \frac{1}{K}\ell n\frac{yU_\tau}{\nu} + \text{const}$$

where K was taken to be 0.4 and $U_\tau = \sqrt{\tau_w/\rho_w}$.

III. Results and Discussion

Experimental results used to evaluate the test apparatus as well as results indicative of the SBLI region for cruise conditions will be presented. The boundary-layer measurements were obtained at $M=0.76$ with a shock Mach number of 1.22 which corresponds to an airfoil pressure distribution where the airfoil is slightly into drag rise. Data will be presented from 40 to 60% chord in increments of 5% chord.

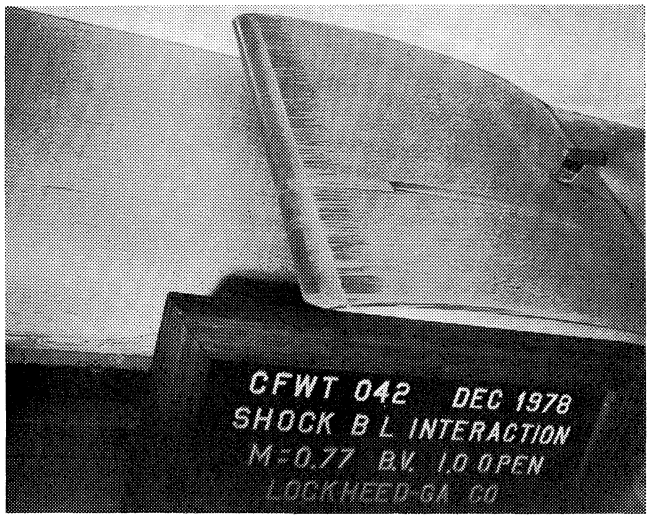

Fig. 10 Oil flow visualization at $M=0.78$, $R_{N_c}=11\times10^6$.

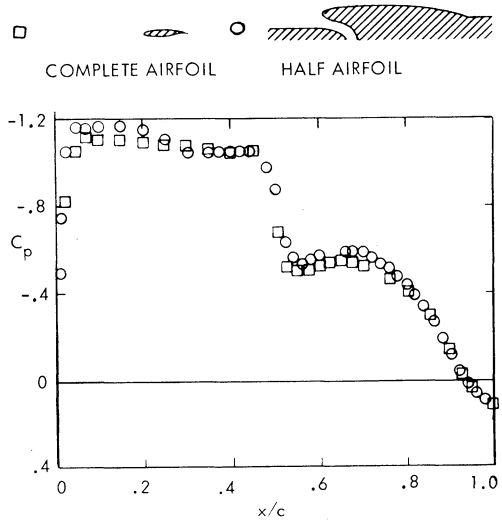

Fig. 11 Comparison of airfoil pressure distribution at cruise conditions, $M_\infty=0.75$, $R_{N_c}=11\times10^6$.

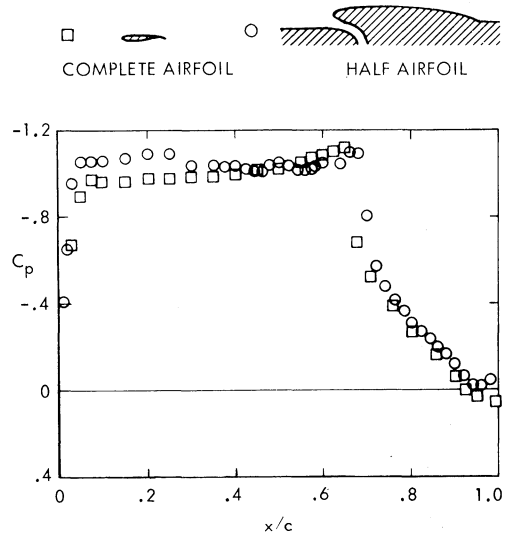

Fig. 12 Comparison of airfoil pressure distributions at shock-induced separation conditions, $M_\infty=0.78$, $R_{N_c}=11\times10^6$.

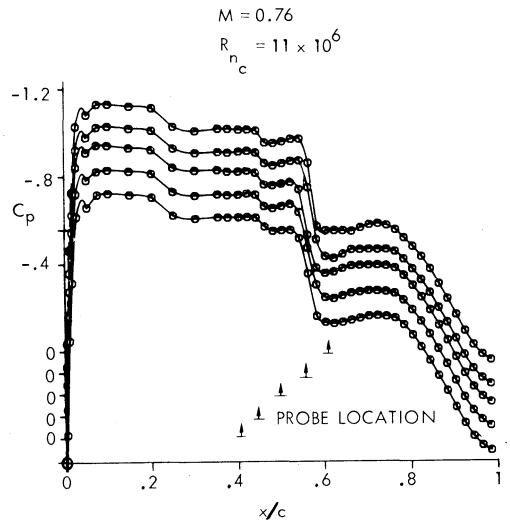

Fig. 13 Airfoil pressure distribution for boundary-layer runs.

The flowfield and bleed duct measurements that were made have not been included in this shock/boundary-layer interaction discussion because the data primarily support Navier-Stokes computations for this particular flow geometry.

Evaluation of Test Apparatus

Since two-dimensionality was a necessary condition for the experiment, a preliminary evaluation of the flow was made by flow visualization. A typical surface oil flow pattern is shown in Fig. 10. The flow over the airfoil can be seen to be very smooth and two-dimensional. The airfoil shock-wave is located near the probe support stem and is straight across the span. Ahead of the airfoil, the flow over the tunnel floor boundary-layer removal duct can also be seen to be smooth and two dimensional.

The half-airfoil apparatus was designed to provide the same flowfield and boundary-layer development over the half-airfoil upper surface as would be encountered on a complete airfoil. Therefore, it is necessary that the half-airfoil develop the same pressure distribution as the complete airfoil. In Fig. 11, a comparison of the 20-in. chord half-airfoil and 7-in. chord complete airfoil pressure distributions is made for a cruise condition of $M=0.75$ and a chord Reynolds number of 11 million. A very close correspondence between the data for two tests is observed.

As freestream Mach number is increased to $M=0.78$, a classic "type B" separation occurs on the LG4-612 airfoil. This is produced by the interaction between the airfoil shock-wave and the boundary layer causing a separation bubble which thickens the boundary layer enough to produce a trailing-edge separation (see Fig. 5). A comparison of the half-airfoil and complete-airfoil pressure distributions under these conditions is shown in Fig. 12. Again, good correspondence is shown between the two sets of data.

The data in Figs. 11 and 12 indicate that the concept of using a large chord half-airfoil to simulate the boundary layer on the smaller complete model is justified. The two airfoils have very similar pressure distributions, including such important quantities as shock location and trailing edge pressure recovery. Since tunnel conditions were set so that Reynolds number based on chord was the same for both models (11×10^6), development of the boundary layer should be similar. It is anticipated that the data obtained from the half-airfoil boundary layer will be directly applicable to the complete model for which the performance characteristics are known, thereby enhancing the understanding of the impact of shock/boundary-layer interaction on supercritical airfoil performance.

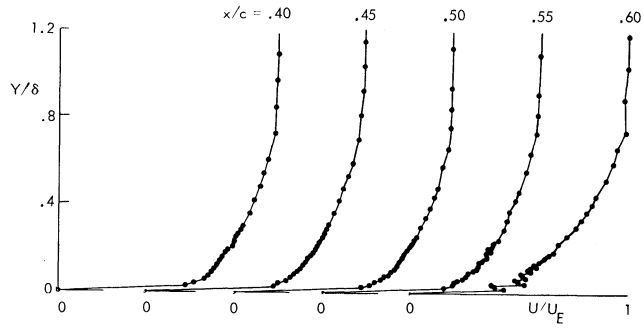

Fig. 14 Velocity profiles.

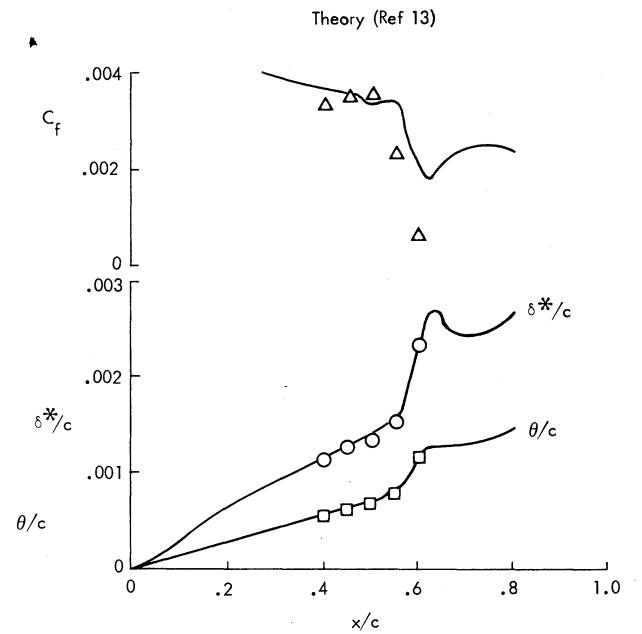

Fig. 15 Comparison of measured boundary layer parameters with theory.

Boundary Layer Measurements

The Lockheed-Georgia Company CFWT is a blow-down wind tunnel, so each boundary-layer traverse is obtained in a separate tunnel run. When building a summary of boundary-layer measurements, the first point to check is to make sure that the airfoil pressure distribution is the same for all runs in the summary. Figure 13 contains the pressure distributions for all five runs in this summary. The C_p scale is displaced to separate the data for clarity. The pressure distribution remains quite consistent from run to run ahead of the shock. A slight change in pressure distribution can be seen downstream of the shock which is caused by very slight variation in tunnel Mach number. Under these conditions, the boundary layer is close to developing a separation bubble which changes the pressure distribution downstream of the shock. The probe location for each run is indicated on the pressure distribution. For example, the $x/c = 0.60$ probe location was used with the top pressure distribution in Fig. 13.

Boundary-layer velocity-profile data obtained during the five runs shown in Fig. 13 are presented in Fig. 14. The first three profiles are typical turbulent boundary-layer profiles which show no effect of the shock wave. The $x/c = 0.55$ profile which is slightly into the pressure rise begins to show the retarding effect of the adverse pressure gradient. The last profile shows the substantial effect of the adverse pressure gradient. Close to the airfoil surface, where the separation bubble will form, the flow has become erratic, with some fluctuations exceeding the 150 ms settling time used at each point.

Boundary-layer integral parameters were computed from these velocity profiles. Growth of displacement thickness through the adverse pressure gradient is shown in Fig. 15. Growth of the displacement thickness is modest ahead of the pressure rise, but then abruptly increases through the shock wave. Growth of the momentum thickness through pressure rise shown in Fig. 15 follows the same pattern.

Skin friction coefficients were deduced from the velocity profiles by plotting the profiles in the law of the wall form. The data contained a substantial logarithmic region except for the $x/c = 0.60$ case where the velocities near the wall were erratic. Skin friction coefficients shown in Fig. 15 were obtained from the slope of the linear part of the logarithmic plot. The result for the $x/c = .60$ case is somewhat uncertain because of the data scatter near the wall.

As a check of the test data, the pressure distribution of Fig. 13 was run in the McNally[13] boundary-layer code. The computed integral parameters are shown in Fig. 15. The agreement is very good for both displacement and momentum thickness. Disagreement of skin friction coefficient with theory in the shock region is not surprising because of the difficulties of obtaining skin friction from velocity profiles under adverse pressure gradient conditions.

Concluding Remarks

A long-term experimental program is underway at the Lockheed-Georgia Company to provide the needed data-base to support development of advanced theoretical methods for prediction of shock/boundary-layer interaction at transonic speeds on supercritical airfoils.

A unique experimental apparatus for obtaining fundamental shock/boundary-layer data has been developed. This apparatus included a half-airfoil model mounted on the wind-tunnel floor and associated instrumentation for measuring the boundary layer on the airfoil and static pressures on all airfoil and tunnel boundaries.

Initial tests of this apparatus at transonic Mach numbers have shown that the apparatus exhibits all of the flow properties peculiar to supercritical airfoils needed for shock/boundary-layer interaction research.

Measurements of the boundary-layer properties of the supercritical airfoil at cruise condition have been presented. These measurements of the boundary layer for a shock wave with a local Mach number only slightly higher than $M = 1.2$ show a substantial growth of the boundary layer through the shock/boundary-layer interaction region. Measured boundary-layer parameters compare well with theoretical calculations under these conditions.

Future research will include the correlation of the experimental shock/boundary-layer interaction data with advanced theoretical codes and the expansion of the experimental data-base to include measurements at high values of Reynolds number, measurements of turbulent velocity fluctuations, and measurements at conditions where separation effects are significant.

Acknowledgments

The author wishes to express his appreciation to Dave Dye, Grady Henrich, and Gerald Pounds for their outstanding efforts in this test program and to Micky Blackwell, Spiro Lekoudis, Eric Robinson, Dave Schuster, Andy Srokowski, and Andy Thomas for their assistance in preparation of this paper.

References

[1] MacCormack, R. W., "An Efficient Numberical Method for Solving the Time-Dependent Compressible Navier-Stokes Equations at High Reynolds Numbers," NASA TM X873, 126, July 1976.

[2] Seddon, J., "The Flow Produced by Interaction with a Normal Shock Wave of Sufficient Strength to Cause Separation," ARC R&M 3502, 1967.

[3]Vidal, R. J., Whittliff, C. E., Catlin, P. A., and Sheen, B. H., "Reynolds Number Effects on the Shock Wave-Turbulent Boundary Layer Interaction at Transonic Speeds," AIAA Paper 73-661, July 1973.

[4]Kooi, J. W., "Experiment on Transonic Shock-Wave Boundary-Layer Interaction," AGARD CP-168, 1975.

[5]Abbiss, J. B., East, L. F., Nash, C. R., Parker, P., Pike, E. R., and Sawyer, W. G., "A Study of the Interaction of a Normal Shock Wave and a Turbulent Boundary Layer Using a Laser Anemometer, RAE TR 75141, 1976.

[6]Mateer, G. G., Brosch, A., and Viegas, J. R., "Normal Shock Wave Turbulent Boundary Layer Interaction at Transonic Speeds," AIAA Paper 76-161, Jan. 1976.

[7]Alber, E. E., Bacon, J. W., and Masson, B. S., "An Experimental Investigation of Turbulent Transonic Viscous-Inviscid Interactions," AIAA Paper 71-565, June 1971.

[8]Lo, C. F., Heltsley, F. L., and Alstatt, M. C., "A Study of Laser Velocimeter Measurements in a Viscous Transonic Flow," AIAA Paper 76-333, July 1976.

[9]Pearcey, H. H., Osborne, J., and Haines, A. B., "The Interaction Between Local Effects at the Shock and Rear Separation - A Source of Significant Scale Effects in Wind-Tunnel Tests on Aerofoils and Wings," AGARD CP-35, Sept. 1968, pp. 11-1, 23.

[10]Sobieczky, H. and Stanewsky, E., "The Design of Transonic Airfoils Under Consideration of Shock Wave Boundary Layer Interaction," ICAS Paper 76-14, Oct. 1976.

[11]Hurley, F. X., Spaid, F. W., Roos, F. W., Stivers, L. S., and Bandettini, A., "Supercritical Airfoil Flowfield Measurements," *Journal of Aircraft,* Vol. 12, Sept. 1975, pp. 734-744.

[12]Smith, P. R. and Keable, F., "High Reynolds Number Test of a 12 Percent Thick Supercritical Airfoil (Designated LG4-612) at Transonic Mach Numbers," Lockheed-Georgia Company LG75ER0147, Oct. 1975.

[13]McNally, W. D., "Fortran Program for Calculating Compressible Laminar and Turbulent Boundary Layers in Arbitrary Pressure Gradients," NASA TND5681, May 1970.

From the AIAA Progress in Astronautics and Aeronautics Series..

AEROACOUSTICS:

JET NOISE; COMBUSTION ANDCORE ENGINE NOISE—v. 43
FAN NOISE AND CONTROL; DUCT ACOUSTICS; ROTOR NOISE—v. 44
STOL NOISE;AIRFRAME AND AIRFOIL NOISE—v. 45
ACOUSTIC WAVE PROPAGATION;
AIRCRAFT NOISE PREDICTION;
AEROACOUSTIC INSTRUMENTATION—v. 46

Edited by Ira R. Schwartz, NASA Ames Research Center, Henry T. Nagamatsu, General Electric Research and Development Center, and Warren C. Strahle, Georgia Institute of Technology

The demands placed upon today's air transportation systems, in the United States and around the world, have dictated the construction and use of larger and faster aircraft. At the same time, the population density around airports has been steadily increasing, causing a rising protest against the noise levels generated by the high-frequency traffic at the major centers. The modern field of aeroacoustics research is the direct result of public concern about airport noise.

Today there is need for organized information at the research and development level to make it possible for today's scientists and engineers to cope with today's environmental demands. It is to fulfill both these functions that the present set of books on aeroacoustics has been published.

The technical papers in this four-book set are an outgrowth of the Second International Symposium on Aeroacoustics held in 1975 and later updated and revised and organized into the four volumes listed above. Each volume was planned as a unit, so that potential users would be able to find within a single volume the papers pertaining to their special interest.

v.43—648 pp., 6 x 9, illus.	*$19.00 Mem.*	*$40.00 List*
v. 44—670 pp., 6 x 9, illus.	*$19.00 Mem.*	*$40.00 List*
v. 45—480 pp., 6 x 9, illus.	*$18.00 Mem.*	*$33.00 List*
v. 46—342 pp., 6 x 9, illus.	*$16.00 Mem.*	*$28.00 List*

For Aeroacoustics volumes purchased as a four-volume set: $65.00 Mem. $125.00 List

TO ORDER WRITE: Publications Dept., AIAA, 1290 Avenue of the Americas, New York, N.Y. 10019